JACS
JOURNAL OF THE AMERICAN CHEMICAL SOCIETY
Article
pubs.acs.org/JACS

# Ultrafast Photoinduced Interfacial Proton Coupled Electron Transfer from CdSe Quantum Dots to 4,4′-Bipyridine

Jinquan Chen,[†] Kaifeng Wu,[†] Benjamin Rudshteyn,[‡] Yanyan Jia,[†] Wendu Ding,[‡] Zhao-Xiong Xie,[§] Victor S. Batista,*[,‡] and Tianquan Lian*[,†]

[†]Department of Chemistry, Emory University, Atlanta, Georgia 30322, United States
[‡]Department of Chemistry, Yale University, New Haven, Connecticut 06520, United States
[§]State Key Laboratory for Physical Chemistry of Solid Surfaces and Department of Chemistry, College of Chemistry and Chemical Engineering, Xiamen University, Xiamen, 361005, China

Supporting Information

**ABSTRACT:** Pyridine and derivatives have been reported as efficient and selective catalysts for the electrochemical and photoelectrochemical reduction of $CO_2$ to methanol. Although the catalytic mechanism remains a subject of considerable recent debate, most proposed models involve interfacial proton coupled electron transfer (PCET) to electrode-bound catalysts. We report a combined experimental and theoretical study of the photoreduction of 4,4′-bipyridium (bPYD) using CdSe quantum dots (QDs) as a model system for interfacial PCET. We observed ultrafast photoinduced PCET from CdSe QDs to form doubly protonated $[bPYDH_2]^{+\bullet}$ radical cations at low pH (4−6). Through studies of the dependence of PCET rate on isotopic substitution, pH and bPYD concentration, the radical formation mechanism was identified to be a sequential interfacial electron and proton transfer (ET/PT) process with a rate-limiting pH independent electron transfer rate constant, $k_{int}$, of $1.05 \pm 0.13 \times 10^{10}$ $s^{-1}$ between a QD and an adsorbed singly protonated $[bPYDH]^+$. Theoretical studies of the adsorption of $[bPYDH]^+$ and methylviologen on QD surfaces revealed important effects of hydrogen bonding with the capping ligand (3-mercaptopropionic acid) on binding geometry and interfacial PCET. In the presence of sacrificial electron donors, this system was shown to be capable of generating $[bPYDH_2]^{+\bullet}$ radical cations under continuous illumination at 405 nm with a steady-state photoreduction quantum yield of 1.1 ± 0.1% at pH 4. The mechanism of bPYD photoreduction reported in this work may provide useful insights into the catalytic roles of pyridine and pyridine derivatives in the electrochemical and photoelectrochemical reduction of $CO_2$.

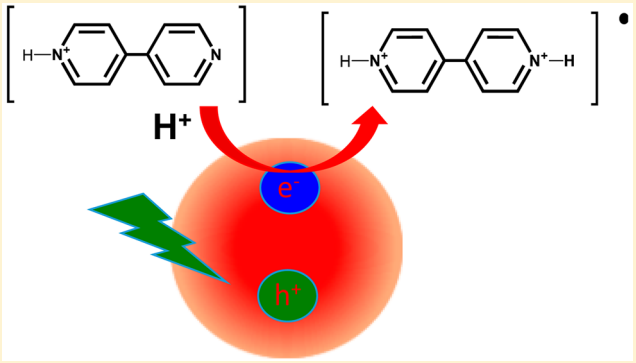


## INTRODUCTION

Photoreduction of $CO_2$ has been intensely studied in recent years, because it is one of the most desirable potential approaches for solar energy conversion and storage.[1] Advancing this field requires major breakthrough in the development of active catalysts for $CO_2$ reduction at low overpotentials.[2] Bocarsly and co-workers have reported efficient and selective conversion of $CO_2$ to methanol in electrochemical (on Pt cathode) and photoelectrochemical (on *p*-type GaP photocathode) cells with pyridine and its derivatives as cocatalysts.[3] More recently, Dyer and co-workers report that 6,7-dimethyl-4-hydroxy-2-mercaptopteridine (PTE) can also function as an electrocatalyst for $CO_2$ reduction using glassy carbon electrodes.[4] These catalysts, operating at relatively low over potentials (−0.65 V vs NHE for pyridine[3] and −0.85 V vs NHE for PTE[4]), are promising candidates for further improvement. However, their mechanisms of $CO_2$ reduction are still a subject of intense debate.[5−8] One of the key steps has been proposed to be reduction of pyridinium to pyridinyl.[5] Because the reduction potential of pyridinium (−1.61 V vs NHE[9]) in aqueous solution is much more negative than the onset potential of electrocatalysis, it has been proposed that the reduction likely involves electrode surface bound species.[5−8] Unfortunately, direct experimental evidence of the existence of the reduced pyridinium radical at electrode surface during $CO_2$ reduction is still lacking.

The aforementioned reactions likely involve interfacial proton-coupled electron transfer (PCET) with the electron delivered by the electrode (electrochemically or photoelectrochemically) and the proton supplied by the solution (which can be freely diffusing in solution, adsorbed on the electrode and/or hydrogen bonded with the catalyst). Although these reactions are essential to electro- and photoelectrocatalysis with heterogeneous catalysts or electrode-attached molecular catalysts, they are much less well understood

**Received:** October 3, 2015
**Published:** December 29, 2015



DOI: 10.1021/jacs.5b10354
J. Am. Chem. Soc. 2016, 138, 884−892

compared to their solution counterparts. In an effort to advance understanding of interfacial PCET and determine its involvement in pyridine-catalyzed $CO_2$ reduction, we have carried out both transient absorption and theoretical studies of CdSe quantum dots (QDs)−bipyridine complexes. 4,4′-bipyridine (bPYD), rather than pyridine, was chosen in this study because it is structurally similar to pyridine and its reduced radical form has a distinct absorption in the visible region that can be directly probed by time-resolved spectroscopy[10] (unlike the UV absorption of pyridinyl radicals[11]). Furthermore, under the pH range (4−7) examined in this work, bPYD molecules (denoting bipyridine in unspecified protonation states) can be in un-, mono- and double-protonated forms (denoted as $bPYD_0$, $[bPYDH]^+$, and $[bPYDH_2]^{2+}$, respectively). The effect of protonation can be conveniently examined by comparing with 1,1′-dimethyl-4,4′-bipyridine, or methylviologen ($MV^{2+}$), which cannot be protonated. We have chosen colloidal CdSe quantum dots to mimic reactions occur on the photoelectrode surfaces (without the involvement of transport issues in bulk electrodes) and to tune the energy of the conduction band electron by their size through the well-known quantum confinement effect.[12−15] Herein, we report the observation of ultrafast photoinduced PCET from CdSe QDs to bPYD molecules to form $[bPYDH_2]^{+\bullet}$ radical cations. By examining the dependence of PCET rates on pH, bPYD concentration and kinetic isotope effect, we showed this reaction occurred via a sequential electron and proton transfer (ET/PT) process to $[bPYDH]^+$ on the QD surface. Theoretical calculations elucidate its binding structure.

## RESULTS AND DISCUSSION

**UV−Vis Absorption Spectra.** Oleic acid (OA) capped CdSe QDs were synthesized according to a literature procedure (see Supporting Information, SI for details).[16] In order to control pH in this study, 3-mercaptopropionic acid (MPA) capped water-soluble QDs were prepared from the oleate capped QDs following a literature ligand exchange procedure.[17] bPYD was added into the QD aqueous solutions to desired concentrations and pH was controlled by adding hydrochloric acid (HCl). Typical UV−vis absorption spectra of QD and QD-bPYD solutions at pH 4 are displayed in Figure 1. The QD solutions exhibited discrete exciton absorption bands with the lowest energy (1S exciton) band at ∼535 nm, which corresponds to an estimated diameter of 2.8 nm.[18] In addition to these QD absorption features, QD-bPYD solutions also exhibited a pronounced absorption from bPYD at ∼300 nm.[19] Both samples showed a long tail after 570 nm due to scattering at low pH conditions when aggregation of QDs appeared. UV−vis absorption spectra of QD and QD-bPYD solutions at other pH values (Figure S1) showed similar features with pH-independent exciton band positions.

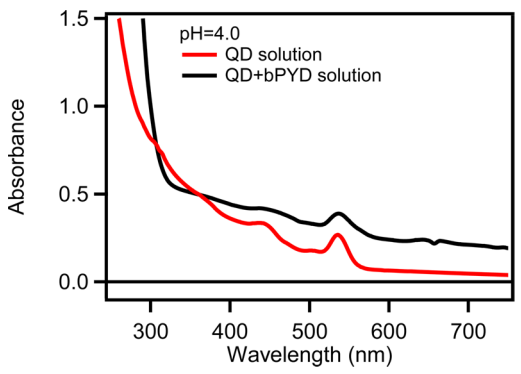


**Figure 1.** UV−vis absorption spectra of CdSe QD solutions with (black) and without (red) bPYD at pH = 4.0.

**Transient Absorption (TA) Study of ET from QD to bPYD.** We first examined the pH dependence of conduction band electron dynamics in QD solutions in the absence of bPYD (referred to as free QDs) by transient absorption spectroscopy with 400 nm excitation. Representative TA spectra of free QDs at pH 4 are shown in Figure 2A and TA spectra at other pHs are shown in Figure S2. These spectra showed a long-lived bleach of 1S exciton band that completely recovered after 100 ns (due to electron and hole recombination). Previous studies have shown that the 1S exciton bleach signal in CdSe QDs can be attributed to the state-filling of the 1S electron level and thus the bleach recovery provides a convenient probe of 1S electron decay dynamics.[20,21] As shown in Figure S2, the 1S electron decay shows negligible pH dependence from pH 4 to 7. These 1S bleach recovery kinetics

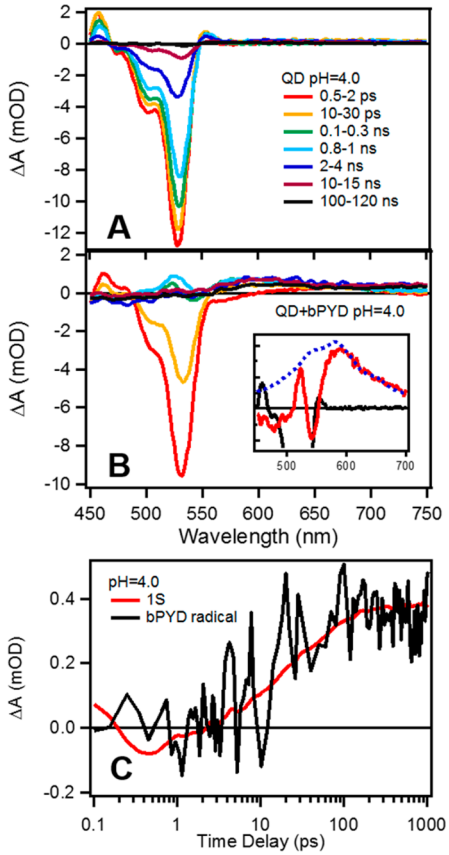


**Figure 2.** Transient absorption spectra of CdSe solutions at pH = 4.0 with (A) 0 mM and (B) 10 mM 4,4′-bipyridine (bPYD) at indicated delay times after 400 nm excitation. The inset in panel B shows an expanded view of average TA spectra at 0.8 to 1 ns of CdSe QDs with (red) and without (black) bPYD. The $[bPYDH_2]^{+\bullet}$ radical cation absorption spectrum is also shown (blue dotted line). (C) Comparison of kinetic traces of 1S exciton bleach recovery (probed at 540 nm) and $[bPYDH_2]^{+\bullet}$ radical cation formation for CdSe-bPYD solutions shown in panel B. The 1S exciton bleach kinetics has been shifted vertically and scaled to allow the comparison of recovery of the bleach with the growth of the radical signal.



DOI: 10.1021/jacs.5b10354
J. Am. Chem. Soc. 2016, 138, 884−892

**Scheme 1. Possible Pathways of Ultrafast Photoinduced Proton Coupled Electron Transfer between CdSe QDs and bPYD**[a]

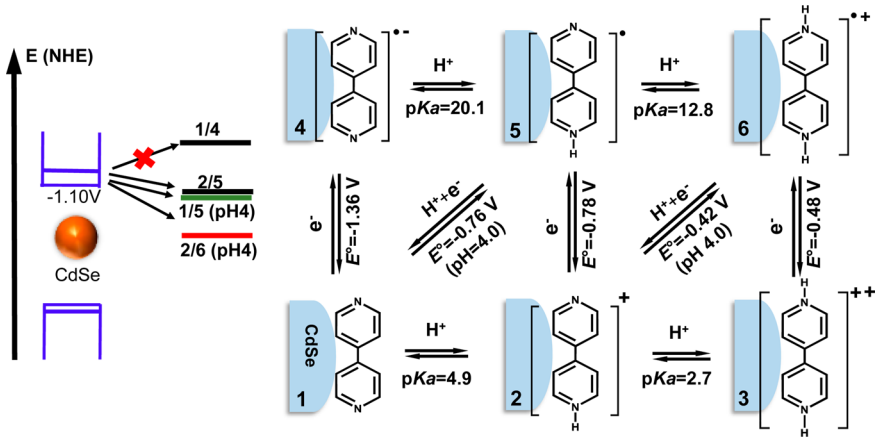


[a]QD 1S electron energy level, p$K_a$ values and reduction potentials vs NHE are adopted from published data.[6,23,24] The different states of bPYD are indicated by bold numerals. **1**/**4** indicates the potential for the conversion of **1** to **4**. **2**/**5** indicates the potential for the conversion of **2** to **5**. **1**/**5** (pH4) indicates the potential for the conversion of **1** to **4** at pH = 4. **2**/**6** (pH4) indicates the potential for the conversion of **2** to **6** at pH = 4. The conduction band edge of CdSe is indicated by the −1.10 V label on the left hand side.

can be fitted by three exponential decay functions with a half-life of 2.2 ± 0.1 ns. Fitting parameters are shown in Table S1. These kinetics as well as the results to be discussed below were measured at low excitation photon fluence ($5.0 \times 10^{-5}$ J/cm$^2$) to ensure negligible contributions of multiexciton states.[22]

Figure 2B shows the transient spectra of a QD-bPYD solution with 10 mM bPYD at pH = 4.0. An expanded view of the average TA spectra with and without bPYD (at 0.8−1 ns) is shown in Figure 2B inset. Compared with free QDs, the 1S exciton bleach recovery of QD-bPYD solution was much faster, indicating shorter-lived 1S electrons. The decay of the 1S electron signal gave rise to the formation of two spectral signatures: a broad adsorbate signal from ∼580 to 700 nm (Figure 2C and Figure S4) and a Stark effect signal of exciton bands. As shown in the inset of Figure 2B, the adsorbate signal agreed well the stable $[bPYDH_2]^{+\bullet}$ radical cation (**6** in Scheme 1) absorption spectrum reported in the literature[10,23,24] and observed in steady-state photoreduction experiment to be discussed below, confirming photoinduced electron transfer from the QD to bPYD molecules. The Stark effect signal, which can be clearly seen after 100 ps, when the 1S electron state filling signal had nearly completely decayed, resembled the first derivative of the absorption spectrum, and has been attributed to the shift of the exciton bands caused by the hole in the QD in the charge separated state.[16] All three spectral signatures (fast exciton bleach recovery, $[bPYDH_2]^{+\bullet}$ radical cation and Stark effect signal formation) confirm photoinduced interfacial ET from the QD to bPYD molecules. Similar TA spectra evolution with increasingly slower rates of PCET spectral signatures (see below) were observed in QD-bPYD solutions at pH = 5.0 and 6.0 and negligible ET signatures were seen at pH 7 (Figure S3).

**pH and bPYD Concentration Dependent Apparent ET Rates.** In QD-bPYD solutions, there exists a bPYD concentration dependent equilibrium between bPYD molecules adsorbed on the QD surface and freely diffusing in solution as well as a distribution of bPYD molecules in different protonation states. To examine whether these reactions occur on the surface of QDs, we have measured the dependence of the PCET rates on bPYD concentration. Representative 1S exciton bleach kinetic traces of QD-bPYD solutions with different bPYD concentrations (from 0 to 20 mM) at pH = 4.0 are displayed in Figure 3A. The apparent bleach recovery rate

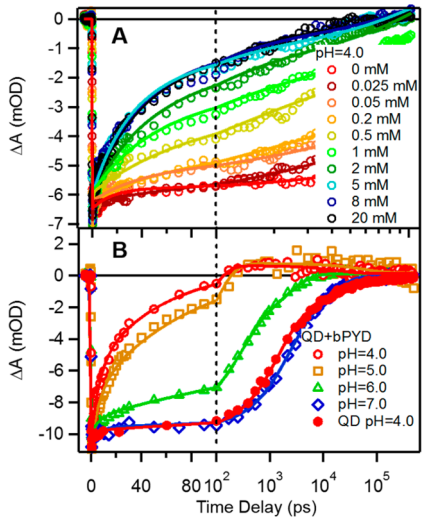


**Figure 3.** 1S exciton bleach recovery kinetic traces (probed at 540 nm) of CdSe-bPYD solutions (A) at pH = 4.0 and indicated bPYD concentrations (B) at indicated pH with 10 mM bPYD. Also shown in (B) is the kinetics of free QDs at pH = 4.0.

($k_{app}$) increased with the concentration of bPYD and it reached a saturated rate at large bPYD concentration. As shown in Figure S5, similar saturation of $k_{app}$ with bPYD concentration was also observed at pH = 5.0 and 6.0. This result suggests that PCET occurs from QD to adsorbed bPYD molecules on the QD surface via static quenching. Similar adsorbate concentration dependent electron and hole transfer kinetics have been reported in previous studies.[17,22,25−27] Although PCET to bPYD molecules in solution (i.e., dynamic quenching) can also occur, this process was excluded for two reasons. First, the rate of this process would increase linearly with the solution concentration and would not saturate at high concentration as was observed in our system.[28,29] Furthermore, a previous study by Weiss and co-workers has shown that dynamic quenching



DOI: 10.1021/jacs.5b10354
J. Am. Chem. Soc. 2016, 138, 884−892

occurs with a much slower rate ($<10^{-6}$ $S^{-1}$) due to presence of native ligands on the QD surface.[29]

To investigate whether the QD-to-bPYD interfacial ET process is coupled with proton transfer, we have measured the pH dependence of the electron transfer kinetics in QD-bPYD solutions (with 10 mM bPYD). Compared with the free QD solutions, the 1S bleach recovery of QD-bPYD solutions showed a systematically longer half-life as pH increased from 4.0 to 7.0, suggesting that $k_{app}$ decreased at higher pH. The half-life was 20 ± 5 ps, 61 ± 6 ps and 292 ± 15 ps at pH = 4.0, 5.0 and 6.0, respectively. At pH 7.0, the kinetic trace of the QD-bPYD solution was similar to that of the free QD (half-life of 2.2 ns), indicating negligible electron transfer at this condition.

**Mechanism of Ultrafast Interfacial PCET.** Photogeneration of $[bPYDH_2]^{+\bullet}$ (**6**) radical cations involves the transfer of an electron from the QD conduction band and protons from the aqueous solution. Possible pathways of concerted (CEPT) and sequential (ET-PT and PT-ET) PCET as well as ET are illustrated in Scheme 1. The energetics of the 1S electron in QDs can be estimated according to published procedures from the reported bulk band edge position (−0.7 V vs NHE)[30] and size dependent quantum confinement energy.[12] For CdSe QDs with an 1S exciton band at 535 nm, the estimated reduction potential for the QD excited state oxidation $QD(1S_e,1S_h)/QD^+(1S_h)$ is −1.10 V vs NHE. Because of the lone pair electrons on the nitrogen atom, bipyridine can exist in unprotonated ($bPYD_0$, **1** in Scheme 1) as well as mono- ($[bPYDH]^+$, **2**) and double- ($[bPYDH_2]^{2+}$, **3**) protonated forms. The fractions of these species in pH 4−7, calculated according to the reported $pK_{a1}$ (4.9) and $pK_{a2}$ (2.7) values at 298 K,[31] are listed in Table 1. In pH 4−6 where PCET was

**Table 1. Fraction of Un- (1), Mono- (2) and Double- (3) Protonated bPYD at Different pH**

| pH | $bPYD_0$ (**1**) fraction (%) | $[bPYDH]^+$ (**2**) fraction (%) | $[bPYDH_2]^{2+}$ (**3**) fraction (%) |
|---|---|---|---|
| 4.0 | 10.7 | 85.0 | 4.3 |
| 5.0 | 55.6 | 44.2 | 0.2 |
| 6.0 | 92.6 | 7.4 | <0.01 |
| 7.0 | 99.2 | 0.8 | ≪0.01 |

observed, the **1** and **2** forms dominate. Because of the small concentration of **3**, major contributions from direct ET pathway (**3**−**6**) can be ruled out even though it is energetically allowed. Furthermore, according to Table 1, from pH = 4.0 to 5.0, the fraction of **3** decreases by 20-fold, while the observed bleach recovery (ET) rate only decreases by 2-fold (Table S1), inconsistent with the expected ET rate change if **3** to **6** is the main pathway. Direct reduction of **1** followed by two sequential protonation steps (**1**−**4**−**5**−**6**) is not energetically allowed, because of the large reduction potential of **1** (−1.36 V vs NHE). The remaining possible pathways for forming **6** are the concerted CPET (**1**−**5**−**6**, and **2**−**6**) and sequential ET-PT (**2**−**5**−**6**).

The best method to identify CPET pathway is by observing a kinetic isotope effect (KIE).[32] KIE in CPET at the low-frequency limit is given by eq 1.[32]

$$\mathrm{KIE} = \frac{|S_H|^2}{|S_D|^2}\exp\left\{-\frac{2k_BT}{M\Omega^2}(\alpha_D^2 - \alpha_H^2)\right\} \quad (1)$$

Here $M$ and $\Omega$ are the effective mass and frequency, $\alpha$ is the equilibrium donor−acceptor distance, $S_H$ ($S_D$) is the proton (deuteron) transfer overlap between a given pair of proton (deuteron) donor−acceptor vibronic states at the equilibrium distance. Because $S_H$ is typically substantially larger than $S_D$ due to the smaller mass of a proton, a significant KIE is expected in CPET. Shown in Figure 4 is the comparison of 1S exciton

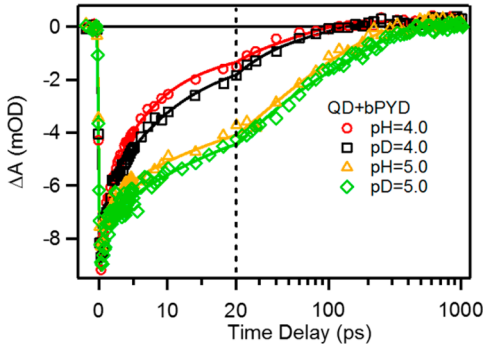


**Figure 4.** Comparison between 1S exciton bleach recovery kinetics (probed at 540 nm) of QD-bPYD (with 10 mM bPYD) in $H_2O$ and $D_2O$ solutions at indicated pH (pD) values.

bleach recovery kinetics for QD-bPYD in $H_2O$ and $D_2O$ solutions at pH (pD) 4 and 5 measured under the same excitation conditions. These kinetic traces were almost identical (see fitting parameters in Table S2) at the same pH and pD. From the measured half-life the KIE values were calculated to be 1.07 ± 0.07 and 1.02 ± 0.02 at pH 4 and 5, respectively, indicating negligible KIE for ET from QD to bPYD.

The lack of KIE in the ET process in QD-bPYD solutions excludes pathways involving concerted CPET, i.e., **2** to **6** and **1** to **5** in Scheme 1. The only remaining pathway for the observed ultrafast interfacial PCET in QD-bPYD solution is the sequential ET-PT channel: ET (**2**−**5**) followed by PT (**5**−**6**). It has been shown previously that $[bPYDH]^{\bullet}$ (**5**) has an absorption band centered at ∼540 nm, blue-shifted from that of **6**.[10] Although in principle the formation kinetics **5** can be monitored to directly follow the PT (**5**−**6**) step, this measurement was hindered by the overlap of this signal with the much larger exciton bleach at the same wavelength (Figure 2B). Instead, we compared the kinetics of radical formation at 560−600 nm (where both **5** and **6** absorb) and at 620−650 nm (where **5** has negligible contribution) in Figure S4a. The comparison shows similar kinetics at these wavelengths, suggesting much smaller concentration of **5** compared to **6** during the PCET process and the radical signal is dominated by **6**. Furthermore, as shown in Figure 2C and Figure S4, the comparison of the $[bPYDH_2]^{+\bullet}$ (or $[bPYDD_2]^{+\bullet}$) formation signals and the 1S bleach recovery in $H_2O$ (or $D_2O$) show that the kinetics of the 1S exciton bleach recovery matched well with the formation of the double protonated radical anion. These results suggest that the overall kinetics of product formation (**2**−**6**) is limited by the electron transfer step (**2**−**5**) and that proton transfer (**5**−**6**) is much faster than electron transfer (**2**−**5**) in this system. Indeed, from pH 4 to 5, the concentration of protons decreases by 10-fold while the apparent ET-PT rate decrease by only 2-fold, which is also consistent with PT not being the rate-limiting step.

As will be shown later, ET half-life ranges from 20 ps at pH = 4 to 292 ps at pH = 6 (Table S1), suggesting that protonation of **5** occurs on a much faster time scale. Assuming a diffusion-limited reaction rate constant of $10^{11}$ $M^{-1}$ $S^{-1}$, the pseudo-first-order rate constant of 5 protonation can be estimated to be $10^7$


DOI: 10.1021/jacs.5b10354
J. Am. Chem. Soc. 2016, 138, 884−892

$S^{-1}$ at pH 4 and $10^5$ $S^{-1}$ at pH 6.[33,34] These diffusion limited rates are much slower than the observed protonation rate. Previous studies have shown that proton transfer can occur on the subpicosecond time scale if the proton donor is hydrogen bonded to the acceptor.[33] We hypothesize that there likely exists a hydrogen bond between $[bPYDH]^+$ (**2**) and a proton donor to allow an ultrafast PT process. This hypothesis appears to be supported by a computational study to be discussed below, which shows that $[bPYDH]^+$ is likely hydrogen-bonded to a proton on the COOH group of the MPA capping ligand on the QD surface.

**pH-Independent Intrinsic ET Rate Constant ($k_{int}$) from QD to $[bPYDH]^+$.** As shown in Figure 3A, the apparent ET-PT rate ($k_{app}$) from QD to $[bPYDH]^+$ depends on the total concentration of bPYD. Since ET/PT (**2**−**5**−**6**) is the only viable pathway, this likely reflects the concentration and pH dependent change of the number of adsorbed $[bPYDH]^+$ molecules. For a QD with $n_1$ adsorbed $[bPYDH]^+$ molecules, apparent ET rate is given by

$$k_{app} = -n_1 k_{int} \tag{2}$$

Here, $k_{int}$ is the intrinsic ET-PT rate constant between a QD and an adsorbed $[bPYDH]^+$. Because $n_1$ changes with the total bPYD concentration and solution pH, we need to determine $k_{int}$ from the apparent ET rates to allow a meaningful comparison of ET-PT rates measured under different pH.

Extensive previous single QD[35−37] and ensemble-averaged studies[25,26,38] showed that adsorption of acceptors on QD surfaces follow a Poisson distribution. The probability of finding QDs with $n_i$ adsorbed species $i$ ($i$ = 0 for bPYD, $i$ = 1 for $[bPYDH]^+$) molecules is

$$P(n_i, m_i) = \left(\frac{m^{n_i} e^{-m_i}}{n_i!}\right) \tag{3}$$

where $m_i$ is the average number of adsorbed species $i$. Following previous models of fluorescence quenching kinetics in micelles,[39−41] the ensemble averaged 1S exciton bleach recovery kinetics can be shown to be given by[25,26,38]

$$N(t, m_1) = N(0)\left(\sum_n e^{-n_1 k_{int} t} P(n_1, m_1)\right) S_{free}(t)$$
$$= N(0)\left(e^{m_1[e^{-k_{int}t}-1]}\right) S_{free}(t) \tag{4}$$

where $N(t,m_1)$ and $N(0)$ and population at time $t$ and 0, and $S_{free}(t)$ is the bleach recovery kinetics of free QDs (without bPYD). $S_{free}(t)$ was independently determined by fitting the free QD kinetics by three exponential decay functions (Table S4A). Eq 4 was then used to globally fit the adsorbate concentration dependent kinetics (Figure 3A, S5, S6 and S8) with $k_{int}$ (same at a given pH) and $m_1$ as the only fitting parameters. The obtained $k_{int}$ and $m_1$ values are listed in Table S4B.

The $m_1$ values obtained from the fit of two separated bPYD concentration dependent kinetics are plotted as a function of total bPYD concentration in solution in Figure 5A. The adsorbed number of $bPYD_0$, and $[bPYDH]^+$ on QD surface should follow the competitive adsorption Langmuir adsorption isotherm (eq 5).[26]

$$\theta_1 = \frac{m_1}{A_0} = \frac{K_1 f_1 [bPYD]}{1 + K_0 f_0 [bPYD] + K_1 f_1 [bPYD]} \tag{5}$$

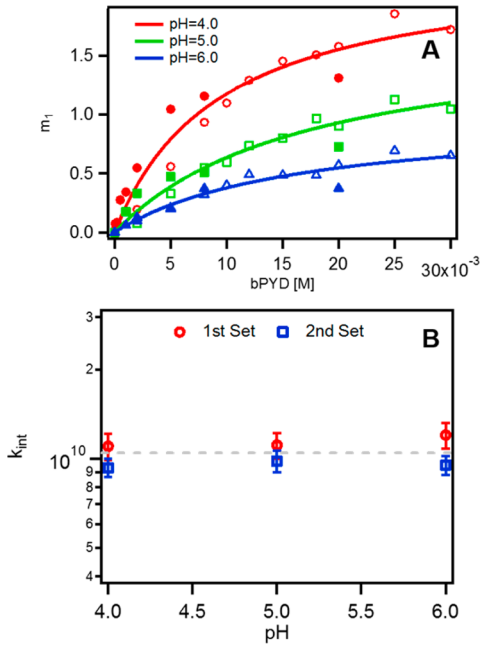


**Figure 5.** (A) The average number ($m_1$) of adsorbed $[bPYDH]^+$ on CdSe QDs as a function of free bPYD in solution (solid symbols are the first set of data and hollow symbols are the second set of data; solid line is the Langmuir fit). (B) The intrinsic electron transfer rate ($k_{int}$) at different pH values from two separate sets of data (gray dashed line is for guidance).

Here $\theta_1$ is the mean fractional surface coverage of $[bPYDH]^+$ species on QDs, $A_0$ is the total number of available adsorption sites per QD, $K_0(f_0)$ and $K_1(f_1)$ are the binding constant (fraction in solution) of $bPYD_0$, and $[bPYDH]^+$ under certain pH. Figure 5A was fit by eq 5, from which we obtained $A_0$, $K_0$ and $K_1$ (see Table S3). The fit reveals that the binding constant is similar from pH 4 to 6, and its value for $bPYD_0$ ($50 \pm 8$ $M^{-1}$) is smaller than for $[bPYDH]^+$ ($112 \pm 7$ $M^{-1}$). The fits also revealed an available adsorption site ($A_0$) value of ~2 (Table S3), which corresponds to about 0.38% of all surface $Cd^{2+}$ atoms (estimated to be 450 for a QD of 2.8 nm diameter[26]).

$k_{int}$ values obtained from the fit agree with each other within experimental errors for pH 4−6 in the two separated bPYD concentration dependence kinetics as shown in Figure 5B. It revealed an average intrinsic ET-PT rate constant from QDs to $[bPYDH]^+$ of $1.05 \pm 0.13 \times 10^{10}$ $s^{-1}$ that was independent of pH, consistent with ET process being the rate limiting step. The analysis above suggests that the intrinsic ET-PT rate from QDs to $[bPYDH]^+$ is independent of pH and the observed variation of the apparent ET-PT rates with the concentrations of bPYD and pH can be accounted for by the change of the number of adsorbed $[bPYDH]^+$ molecules on QD surface. It implies a negligible pH dependence of QD conduction band edge position and QD/adsorbate electronic coupling strength. The latter is also consistent with the negligible pH dependence of binding constant obtained from the Langmuir isotherm analysis discussed above.

To provide further support of this model, we have also measured concentration and pH dependence of ET rates from QD to $MV^{2+}$, which cannot be protonated due to the presence of methyl groups on the N atoms. For QD-$MV^{2+}$ solutions at pH = 4.0 and 7.0, identical ET kinetics (Figure S7 and S8) were observed at the same $MV^{2+}$ concentration. These data can be well fit by eq 4 to obtain $k_{int}$ of 4.63 ($\pm$0.18) $\times 10^{11}$ $s^{-1}$ at pH 4


DOI: 10.1021/jacs.5b10354
J. Am. Chem. Soc. 2016, 138, 884−892

and 4.57 (±0.21) × $10^{11}$ $s^{-1}$ at pH 7 (Table S4B). The average number of adsorbed $MV^{2+}$ as a function of $MV^{2+}$ concentration can also be fit by Langmuir isotherm to obtain a binding constant of 1093 ± 350 $M^{-1}$ at pH 4 and 1292 ± 400 $M^{-1}$ at pH 7 (Table S3).[26,42] These results also suggest the adsorbate/QD interaction and ET rates are independent of pH, providing further support for the pH-independent intrinsic ET-PT rate and binding constant obtained for QD-$[bPYDH]^+$. It is interesting to note that the binding constants increase from $bPYD_0$, $[bPYDH]^+$, and $MV^{2+}$, correlating with a trend of positive charges of these adsorbate.

**pH-Dependent Steady-State Photoreduction Quantum Yield of bPYD.** Photoreduction of bPYD at different pH were performed following a similar protocol reported for $MV^{2+}$.[17] QD-bPYD anaerobic solutions with 10.0 mM bPYD were prepared similarly to those for the transient measurements. Excess (50 mM) MPA was added as sacrificial electron donors and the pH of the solutions was adjusted to desired values by adding NaOH and HCl. The QD concentrations were adjusted to ensure that all solutions had the same absorbance at the illumination wavelength (0.5 OD at 405 nm). As shown in Figure 6A, upon illumination of QD-bPYD sample at pH = 4.0,

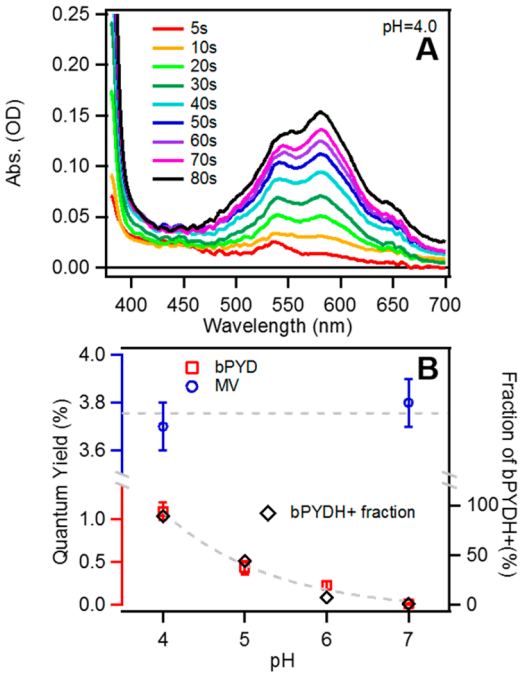


**Figure 6.** Steady-state photoreduction of bPYD. (A) UV−vis difference spectra (after−before irradiation) of a solution containing CdSe QD, 10 mM bPYD and 50 mM MPA after indicated time of irradiation, showing the generation of $[bPYDH_2]^{+\bullet}$ radical cation. Similar spectra at different pH values are shown in Figure S9 and S10. (B) Initial quantum yields of $[bPYDH_2]^{+\bullet}$ (red open squares) and $MV^{+\bullet}$ (blue open circlcs) radical cation generation at different pH values. Also shown is the fraction of $[bPYDH]^+$ in solution as a function of pH (right-hand *y* axis).

bPYD radicals quickly formed, as indicated by the growth of a distinct 580 nm band in the difference spectra. This absorption band matched well with the reported absorption of the stable $[bPYDH_2]^{+\bullet}$ radical cation.[10,24,23] Complete sets of steady-state UV−vis difference spectra for all studied pH are shown in Figure S9.

Using the reported extinction coefficient (13500 ± 200 $M^{-1}$ $cm^{-1}$ at 580 nm),[10] the amounts of $[bPYDH_2]^{+\bullet}$ radical cations as a function of illumination time were calculated to construct the radical formation kinetics (Figure S11). The photon-reduction quantum yields of bPYD is defined in eq 6.

$$\Phi_{bPYD} = \frac{v([bPYDH_2]^{+\bullet})}{v(h\nu)} \quad (6)$$

where $v([bPYDH_2]^{+\bullet})$ is the $[bPYDH_2]^{+\bullet}$ radical cation generation rate (which is the slope of $[([bPYDH_2]^{+\bullet}]$ vs time plots shown in Figure S11) and $v(h\nu)$ is the photon absorption rate of the reaction solution, respectively. Due to the consumption of the electron and/or hole acceptors, the rate decreased slowly with time. For this reason, only the initial quantum yields were calculated and compared in Figure 6B. Under our experimental conditions, the measured initial quantum yield was 1.1 ± 0.1% at pH = 4.0 and it decreased to 0.4 ± 0.1% and 0.2 ± 0.1% at pH = 5.0 and 6.0, respectively. At pH = 7.0, no $[bPYDH_2]^{+\bullet}$ radical cations was generated and the quantum yield was set to 0. As a comparison, steady-state photoreduction of $MV^{2+}$ was also carried out under the same condition at pH = 4.0 and 7.0 (Figure S10). The $MV^{+\bullet}$ radical generation quantum yield was (~3.7%), independent of pH. Also shown in Figure 6 is the calculated fraction of $[bPYDH]^+$ in the solution as a function of pH. The decrease of steady-state $[bPYDH_2]^{+\bullet}$ radical generation quantum yield at higher pH follows the same trend as the fraction of monoprotonated $[bPYDH]^+$ species. This is consistent with the observed trend of apparent PCET rates discussed above and may suggest a relationship between these quantities. However, further studies will be needed to uncover this relationship because the overall $[bPYDH_2]^{+\bullet}$ radical generation quantum yields depend on many other parameters, including the rates of charge separation, charge recombination, and hole-filling (by the sacrificial electron donor) processes in the system under the steady-state photoreduction conditions.

The binding modes of and the differing behavior between $[bPYDH]^+$ and $MV^{2+}$ on the surface of the CdSe quantum dot were investigated using DFT calculations with PW91/(LANL2DZ,6-31G) (methods further described in the Supporting Information). The structures of $[bPYDH]^+$ and $MV^{2+}$ were optimized on a small, simplified cluster model of CdSe with two MPA (3-mercaptopropionic acid) anions bound, as shown in Figures 7 and 8 respectively. These optimized structures show that bPYD prefers to hydrogen bond with both MPA anions rather than lay close to the surface, unlike $MV^{2+}$, which cannot due to its methyl groups. Both bPYD and $MV^{2+}$ have their aromatic C−H groups facing the surface. The optimized structure for bPYD shows asymmetrical hydrogen bonding so that only one $H^+$ is bonded to the bPYD (1.22 Å) while the other $H^+$ is merely hydrogen bonding to it (1.59 Å), corroborating the role of $[bPYDH]^+$ in electron transfer. Furthermore, the hydrogen bonding of $[bPYDH]^+$ with MPA also enables ultrafast PT following ET in the observed ET-PT process discussed above. This situation corresponds to a pH around or less than 6 where there is still a substantial amount of protonated MPA molecules ($pK_a$ ~ 6).[43] Thus, the pH dependence of the protonation state of the surface MPA ligands may also contribute to the observed pH dependent apparent ET-PT rates in Figure 3. However, our analysis above suggests that this effect is likely overshadowed by the pH dependent concentration of $[bPYDH]^+$ in solution


DOI: 10.1021/jacs.5b10354
J. Am. Chem. Soc. 2016, 138, 884−892

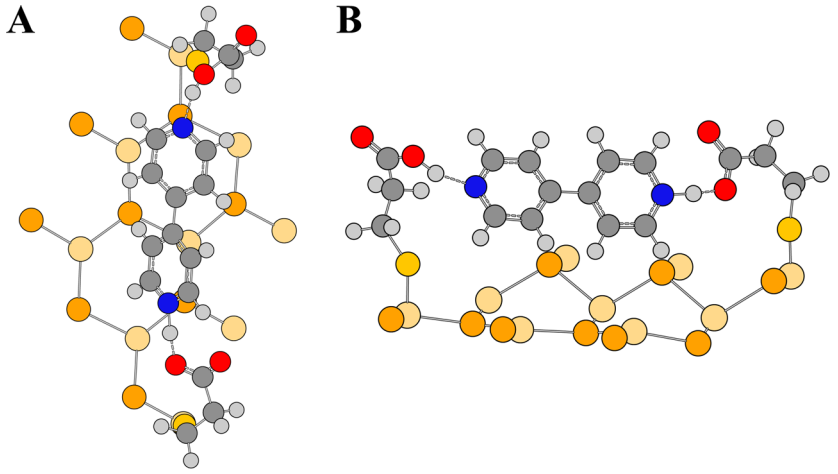


**Figure 7.** Structure of $[bPYDH]^+$ on the CdSe {100} cluster model from above (A) and from the side (B). The color code is as follows: white = H, red = O, gray = C, yellow = S, blue = N, brown = Se, and tan = Cd.

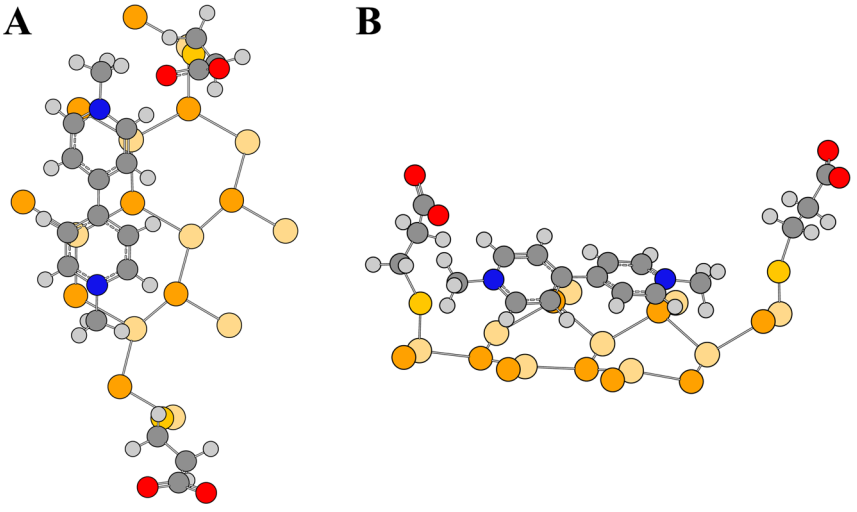


**Figure 8.** Structure of $MV^{2+}$ on the CdSe {100} cluster model as described in Figure 7 for bPYD.

**Scheme 2. The Differing Binding of bPYD (A) and $MV^{2+}$ (B) onto the CdSe Quantum Dot**

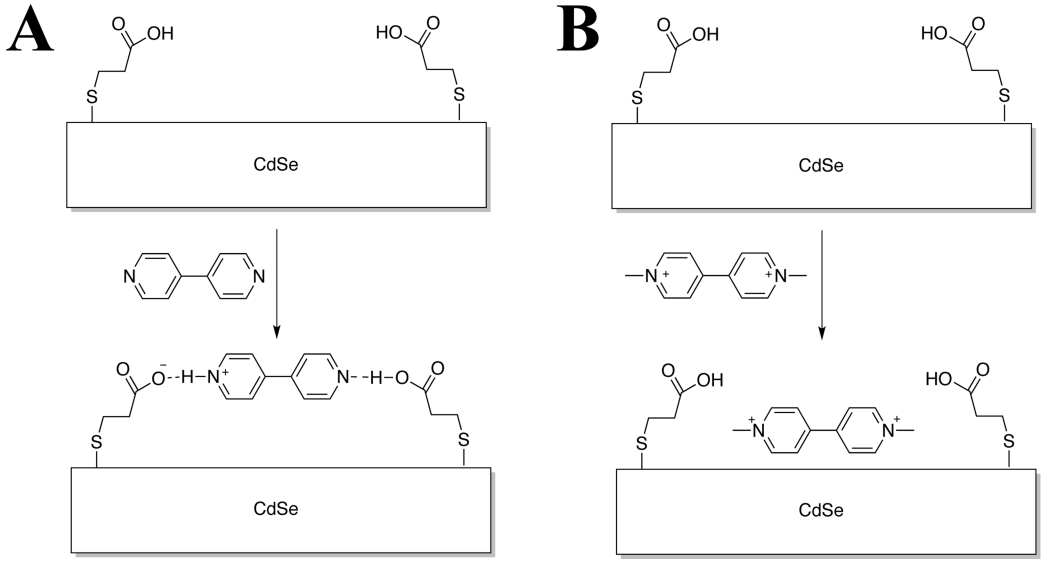


(first and second $pK_a$ are 4.9 and 2.7, respectively, as shown in Scheme 1).

The binding modes depicted in Scheme 2 correspond to a relatively large surface MPA ligand density. Although the exact



DOI: 10.1021/jacs.5b10354
J. Am. Chem. Soc. 2016, 138, 884–892

binding mode of $[bPYDH]^+$ likely depends on the surface ligand density, our geometry optimization indicates a general trend of stabilization by hydrogen bonding of $[bPYDH]^+$ with MPA rather than directly with the Cd or Se on the surface. These results show that $MV^{2+}$ binds closer to the surface than $[bPYDH]^+$ does (a typical aromatic C−Se distance in the former is 2.93 Å while in the latter it is 4.32 Å), which is the likely origin of the faster pH-independent rate of electron-transfer for the former. The hydrogen bonding interaction with the MPA prevents $[bPYDH]^+$ from getting close to the surface as illustrated in Scheme 2A. On the other hand, as illustrated in Scheme 2B, the computational model suggests that the $MV^{2+}$ binding is not as affected by the MPA molecules as it is permanently positively charged and can bind to the surface more efficiently due to increased electrostatic attraction. $MV^{2+}$ is able to bind to the surface as it is most likely as favorably affected by solvation by water as by binding to the surface.

## CONCLUSION

In conclusion, we have observed an ultrafast photoinduced interfacial proton coupled electron transfer process from CdSe QDs to bPYD to form $[bPYDH_2]^{+\bullet}$ radical cations. This process, with negligible kinetic isotope effect, occurred via a sequential electron and proton transfer (ET/PT) process to adsorbed $[bPYDH]^+$ molecules with a rate limiting "intrinsic" electron transfer rate, $k_{int}$, of $1.05 \pm 0.13 \times 10^{10}$ $s^{-1}$ between a QD and an adsorbed $[bPYDH]^+$, slower than for $MV^{2+}$. The apparent PCET rates in QD-bPYD solution increased with total bPYD concentration in solution until a saturation concentration of ∼8 mM. This trend can be well modeled by a concentration dependent surface coverage of $[bPYDH]^+$ according to the Langmuir isotherm. The apparent PCET rates decreased at higher pH and can be attributed to the reduction of the $[bPYDH]^+$ fraction in solution. Direction reduction of $bPYD_0$ (with a reduction of −1.36 V, Scheme 1) is energetically not favorable. The fraction of $[bPYDH_2]^{2+}$ as given in Table 1 is too small, compared to the fraction of $[bPYDH]^+$, to contribute significantly to the observed reaction. Finally, in the presence of sacrificial electron donor (3-mercaptopropionic acid), $[bPYDH_2]^{+\bullet}$ radical cations can be generated under continuous illumination. The steady-state photoreduction quantum yield was $1.1 \pm 0.1\%$ at pH = 4.0 and decreased to $0.2 \pm 0.1\%$ at pH = 6.0, following the trend of the fraction of $[bPYDH]^+$ in solution. Theoretical calculations corroborate the role of $[bPYDH]^+$ in electron injection and suggest that the faster injection into $MV^{2+}$ is due to its ability to bind closer to the surface. Our results provide insight into the photoreduction of bPYD on the surface of semiconductor nanocrystals.

## ASSOCIATED CONTENT

### Supporting Information

The Supporting Information is available free of charge on the ACS Publications website at DOI: 10.1021/jacs.5b10354.

Experimental details include sample preparations, pump−probe transient absorption spectroscopy setup, additional figures of UV−vis absorption, transient absorption spectra and kinetics and photoreduction of bPYD ($MV^{2+}$) at different pH, fitting details of the TA kinetics and Langmuir isotherm. Theoretical details include a description of the methods, the theoretical models superimposed onto the large QD model, and geometry coordinates for theoretical calculations. (PDF)

## AUTHOR INFORMATION


### Corresponding Authors

*E-mail: victor.batista@yale.edu.
*E-mail: tlian@emory.edu.


### Notes

The authors declare no competing financial interest.

## ACKNOWLEDGMENTS

This work was support by the Air Force Office of Scientific Research through grant #FA9550-13-1-0020. B.R. acknowledges support from the National Science Foundation Graduate Research Fellowship under Grant No. DGE-1122492. V.S.B. acknowledges supercomputing time from NERSC and from the Yale High Performance Computing Center.

## REFERENCES


(1) Lewis, N. S.; Nocera, D. G. *Proc. Natl. Acad. Sci. U. S. A.* **2006**, *103*, 15729.
(2) Kumar, B.; Llorente, M.; Froehlich, J.; Dang, T.; Sathrum, A.; Kubiak, C. P. *Annu. Rev. Phys. Chem.* **2012**, *63*, 541.
(3) Barton, E. E.; Rampulla, D. M.; Bocarsly, A. B. *J. Am. Chem. Soc.* **2008**, *130*, 6342.
(4) Xiang, D.; Magana, D.; Dyer, R. B. *J. Am. Chem. Soc.* **2014**, *136*, 14007.
(5) Yan, Y.; Zeitler, E. L.; Gu, J.; Hu, Y.; Bocarsly, A. B. *J. Am. Chem. Soc.* **2013**, *135*, 14020.
(6) Keith, J. A.; Carter, E. A. *J. Am. Chem. Soc.* **2012**, *134*, 7580.
(7) Lim, C.-H.; Holder, A. M.; Musgrave, C. B. *J. Am. Chem. Soc.* **2012**, *135*, 142.
(8) Ertem, M. Z.; Konezny, S. J.; Araujo, C. M.; Batista, V. S. *J. Phys. Chem. Lett.* **2013**, *4*, 745.
(9) Keith, J. A.; Carter, E. A. *Chem. Sci.* **2013**, *4*, 1490.
(10) Simic, M.; Ebert, M. *Int. J. Radiat. Phys. Chem.* **1971**, *3*, 259.
(11) Neta, P.; Patterson, L. *J. Phys. Chem.* **1974**, *78*, 2211.
(12) Brus, L. E. *J. Chem. Phys.* **1984**, *80*, 4403.
(13) Gur, I.; Fromer, N. A.; Geier, M. L.; Alivisatos, A. P. *Science* **2005**, *310*, 462.
(14) Nozik, A. J.; Beard, M. C.; Luther, J. M.; Law, M.; Ellingson, R. J.; Johnson, J. C. *Chem. Rev.* **2010**, *110*, 6873.
(15) Talapin, D. V.; Lee, J. S.; Kovalenko, M. V.; Shevchenko, E. V. *Chem. Rev.* **2010**, *110*, 389.
(16) Zhu, H.; Song, N.; Rodriguez-Cordoba, W.; Lian, T. *J. Am. Chem. Soc.* **2012**, *134*, 4250.
(17) Zhu, H.; Song, N.; Lv, H.; Hill, C. L.; Lian, T. *J. Am. Chem. Soc.* **2012**, *134*, 11701.
(18) Yu, W. W.; Qu, L. H.; Guo, W. Z.; Peng, X. G. *Chem. Mater.* **2003**, *15*, 2854.
(19) Braterman, P. S.; Song, J. I. *J. Org. Chem.* **1991**, *56*, 4678.
(20) Klimov, V. I. *Annu. Rev. Phys. Chem.* **2007**, *58*, 635.
(21) Huang, J.; Stockwell, D.; Huang, Z.; Mohler, D. L.; Lian, T. *J. Am. Chem. Soc.* **2008**, *130*, 5632.
(22) Huang, J.; Huang, Z.; Yang, Y.; Zhu, H.; Lian, T. *J. Am. Chem. Soc.* **2010**, *132*, 4858.
(23) Roullier, L.; Laviron, E. *Electrochim. Acta* **1978**, *23*, 773.
(24) Volke, J.; Volkeová, V. *Collect. Czech. Chem. Commun.* **1972**, *37*, 3686.
(25) Boulesbaa, A.; Issac, A.; Stockwell, D.; Huang, Z.; Huang, J.; Guo, J.; Lian, T. *J. Am. Chem. Soc.* **2007**, *129*, 15132.
(26) Morris-Cohen, A. J.; Frederick, M. T.; Cass, L. C.; Weiss, E. A. *J. Am. Chem. Soc.* **2011**, *133*, 10146.
(27) Wu, K.; Du, Y.; Tang, H.; Chen, Z.; Lian, T. *J. Am. Chem. Soc.* **2015**, *137*, 10224.




DOI: 10.1021/jacs.5b10354
*J. Am. Chem. Soc.* 2016, 138, 884−892

(28) Jiang, Z.-J.; Leppert, V.; Kelley, D. F. *J. Phys. Chem. C* **2009**, *113*, 19161.
(29) Knowles, K. E.; Malicki, M.; Weiss, E. A. *J. Am. Chem. Soc.* **2012**, *134*, 12470.
(30) Berger, L. I. *Semiconductor Materials*; CRC Press: Boca Raton, 1996.
(31) Ashton, L. A.; Bullock, J. I.; Simpson, P. W. *J. Chem. Soc., Faraday Trans. 1* **1982**, *78*, 1961.
(32) Hammes-Schiffer, S.; Stuchebrukhov, A. A. *Chem. Rev.* **2010**, *110*, 6939.
(33) Agmon, N. *J. Phys. Chem. A* **2005**, *109*, 13.
(34) Pérez-Lustres, J.; Rodriguez-Prieto, F.; Mosquera, M.; Senyushkina, T.; Ernsting, N.; Kovalenko, S. *J. Am. Chem. Soc.* **2007**, *129*, 5408.
(35) Issac, A.; Jin, S.; Lian, T. *J. Am. Chem. Soc.* **2008**, *130*, 11280.
(36) Song, N.; Zhu, H.; Jin, S.; Zhan, W.; Lian, T. *ACS Nano* **2010**, *5*, 613.
(37) Jin, S.; Hsiang, J.-C.; Zhu, H.; Song, N.; Dickson, R. M.; Lian, T. *Chem. Sci.* **2010**, *1*, 519.
(38) Huang, J.; Huang, Z.; Jin, S.; Lian, T. *J. Phys. Chem. C* **2008**, *112*, 19734.
(39) Tachiya, M. *J. Chem. Phys.* **1982**, *76*, 340.
(40) Rogers, M. A. J.; Da Silva, M. F.; Wheeler, E. *Chem. Phys. Lett.* **1978**, *53*, 165.
(41) Tachiya, M. *Chem. Phys. Lett.* **1975**, *33*, 289.
(42) Morris-Cohen, A. J.; Vasilenko, V.; Amin, V. A.; Reuter, M. G.; Weiss, E. A. *ACS Nano* **2012**, *6*, 557.
(43) Kim, K.; Kwak, J. *J. Electroanal. Chem.* **2001**, *512*, 83.


DOI: 10.1021/jacs.5b10354
*J. Am. Chem. Soc.* 2016, 138, 884−892